Editors' Suggestion

Tuning spinaron and Kondo resonances via quantum confinement

Markus Aapro,[1,*] Abraham Kipnis,[2,†] Jose L. Lado,[1] Shawulienu Kezilebieke,[3] and Peter Liljeroth[1,‡]
[1]*Department of Applied Physics, Aalto University, FI-00076 Aalto, Finland*
[2]*Department of Neuroscience and Biomedical Engineering, Aalto University, FI-00076 Aalto, Finland*
[3]*Department of Physics, Department of Chemistry and Nanoscience Center, University of Jyväskylä, FI-40014 Jyväskylä, Finland*

(Received 19 January 2024; accepted 18 April 2024; published 6 May 2024)

Controlling zero-bias anomalies in magnetic atoms provides a promising strategy to engineer tunable quantum many-body excitations. Here we show how two different quantum impurities featuring spinaron and Kondo excitations can be controlled via quantum confinement engineering by using circular quantum corrals on a Ag(111) surface. In corrals built from both Ag and Co adatoms, the width of the zero-bias anomaly in the central Co adatom oscillates as a function of corral radius with a period of half of the Ag(111) surface state wavelength. Parameters extracted for Co/Ag(111) show only small differences in the extracted spinaron zero-bias anomaly between corral walls built from Ag or Co adatoms. In quantum corrals occupied by metal-free phthalocyanine, a $S = 1/2$ Kondo system, we observe notable changes in the zero-bias anomaly line shape as a function of corral radius. Our results offer insight into many-body Kondo and spinaron resonances in which the electronic density is controlled by confinement engineering.

DOI: 10.1103/PhysRevB.109.195415

I. INTRODUCTION

The Kondo effect occurs when magnetic impurities are introduced into a nonmagnetic conductor [1]. Local magnetic moments in the impurities interact with the conduction electrons in the nonmagnetic host, resulting in a many-body spin singlet ground state and increasing resistance at low temperatures. The Kondo effect has been studied extensively in bulk and two-dimensional (2D) materials and quantum dot devices [2,3]. There is further interest in observing the Kondo effect in tunneling spectroscopy of single atomic and molecular impurities [4–7].

Low-temperature scanning tunneling microscopy (STM) experiments have demonstrated precise manipulation and placement of surface adsorbates for investigating quantum effects in low-dimensional systems. One of the first examples of this was quantum corrals [8], nanostructures that confine surface state electrons to a two-dimensional geometry, resulting in the formation of confined modes. Their shapes and eigenenergies are determined by the corral shape and size, as well as the surface state dispersion. Engineering the confined modes offers various functionalities [9] such as quantum phase extraction [10], single-atom gating of eigenmode superpositions [11,12], molecular adsorbate tautomerization and manipulation [13,14], and mirage effects [15–17]. Surface state electrons confined to artificial lattices can inherit properties associated with the lattice geometry, such as noninteger dimensionality [18], topological states [19]. and Dirac dispersion [20,21]. The interaction strength between magnetic impurities and electrons in noble metal surface states has been investigated [22–26], and quantum corrals have emerged as a model platform for studying the Kondo effect and its interaction with surface states. Still, details on the coupling between surface states, confined modes, and Kondo impurities remain unresolved. Quantum corrals on Ag(111) offer two benefits over those built on other noble metal surfaces: the confined mode energy widths are small, and due to the surface state onset energy being close to the Fermi energy E_F, it is possible to build corrals with individual (or zero) occupied confined modes.

The cobalt adatom was the first Kondo-like impurity studied with scanning tunneling spectroscopy (STS) [4] and has since been studied on various substrates [27,28] and in quantum corrals [16,22], atomic chains [29,30], and lattices [31]. Many studies have discussed the role of the Ag(111) surface states in the zero-bias anomaly: variations in low-energy spectra have been observed as a function of lateral distance from step edges [22,24], distance from other adatoms [22,29,31], and confinement within quantum corrals and lattices [22,31]. Atomic manipulation was used [25] to map the surface electron density at 3 mV across Ag(111) free from impurities, move a Co adatom around the area, and measure STS at each point to correlate the zero-bias anomaly width to surface state density. This work showed a positive correlation between these variables, suggesting that the zero-bias anomaly can be tuned via the surface state density, further suggesting that the system behaves like a two-channel SU(4) Anderson model rather than a one-channel SU(2) model [25]. It is also important to study how Kondo impurities with different spin states and Anderson model parameters [32] behave in quantum corrals: most studies on Ag(111) have focused only on the Co adatom, which has multiple orbitals contributing to many-body scattering [33].

*Corresponding author: markus.aapro@aalto.fi
†Corresponding author: abraham.kipnis@aalto.fi
‡Corresponding author: peter.liljeroth@aalto.fi

Interestingly, despite its long-standing consideration as a Kondo state, recent studies on the Co/Ag(111) system suggested an alternative explanation for the zero-bias anomaly [34–36]. These studies argued that it arises from gapped spin excitations leading to a spinaron excitation. In contrast to conventional $S = 1/2$ magnetic impurities, the dominant nature of spin excitation in Co stems from the strong magnetic anisotropy of the system due its higher spin. The spinaron is a many-body excitation associated with a magnetic polaron, which arises from the interplay between the spin excitation of the Co and the polarization of the metallic electron cloud. The renewed understanding of the Co zero-bias anomaly motivates the development of strategies to tune and disentangle its microscopic nature and, specifically, contrast it with well-defined Kondo systems.

To compare with the spin excitation and spinaron of Co, a pure $S = 1/2$ magnetic impurity system would be highly desirable. Phthalocyanine (Pc) and its metal complexes have been widely used as individual magnetic impurities due to their chemically stable 2D structure. On adsorption of metal-free H_2Pc molecules on the Ag(111) surface, charge transfer causes the lowest unoccupied molecular orbital (LUMO) to become occupied. Granet *et al.* studied H_2Pc molecules in the dilute limit and in self-assembled monolayers on Ag(111) using STS and ultraviolet photoemission spectroscopy, showing that H_2Pc exhibits the Kondo effect on Ag(111) in both lattices and dilute films [37]. The Kondo peak width, associated with the Kondo temperature of the system, was found to be smaller for H_2Pc molecules in self-assemblies compared to isolated molecules. Similar differences in magnetic behavior have also been observed for H_2Pc on Pb(100), where a single pair of Yu-Shiba-Rusinov states emerges in supramolecular arrays of H_2Pc molecules when the LUMO becomes occupied [38]. The absence of d and f electrons makes the H_2Pc molecule a model system of π magnetism, which has attracted intense research interest [39]. So far, no studies have reported using quantum corrals to explore how modifying the surface state density influences the Kondo effect in H_2Pc/Ag(111).

Here, we use quantum corrals to tune the coupling of Co adatoms and H_2Pc molecules with the Ag(111) surface state and study the corresponding changes in the tunneling spectra to better understand the interactions between magnetic impurities and their electronic environment. We show that the Co atoms confined within corrals on Ag(111) have an oscillating zero-bias anomaly width as a function of corral radius with a period on the order of the Ag(111) surface state Fermi wavelength λ_{E_F} [22]. We further contrast these results with those for a pure $S = 1/2$ Kondo system, providing evidence for the tunability of the H_2Pc molecule Kondo resonance on Ag(111).

II. EXPERIMENT

Our experiments were carried out on an Ag(111) crystal (MaTecK GmbH) cleaned by Ne sputtering (voltage of 1 kV, pressure of 5×10^{-5} mbar) and annealed to 650 °C in UHV ($p < 10^{-9}$ mbar). Atom manipulation and STS were performed at 5 K in two Createc LT-STM/AFM systems equipped with Createc DSP electronics and control software (version 4.4). Co atoms were evaporated from a thoroughly degassed Co wire wrapped around a W filament and deposited directly onto the Ag(111) sample at 5 K. H_2Pc molecules (Sigma Aldrich) were evaporated from a K-cell evaporator at 300 °C onto the substrate at −130 °C.

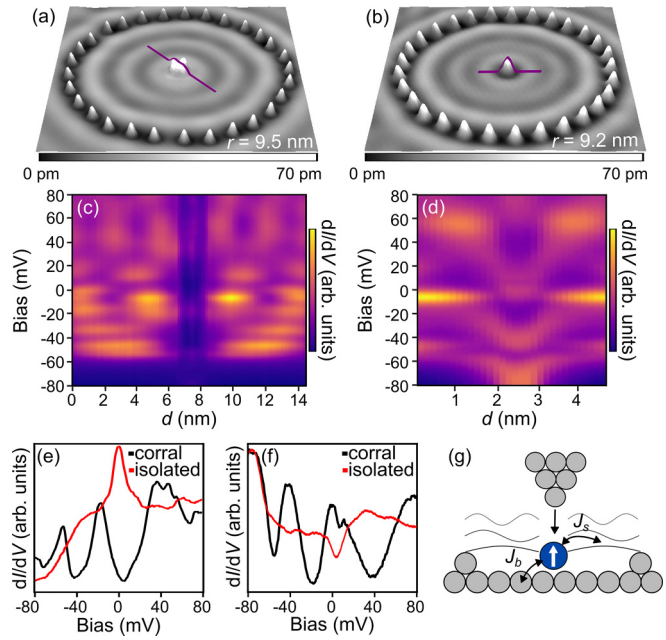

FIG. 1. STM constant-current topography maps of corrals built from Ag adatoms on Ag(111), with a central (a) H_2Pc molecule and (b) Co adatom ($I = 1$ nA, $V = 80$ mV). (c) and (d) dI/dV spectra taken across the purple lines in (a) and (b) ($I = 1$ nA, $V_b = 80$ mV, $V_{\mathrm{mod}} = 1$ mV). The spectra in (c) are normalized by the dI/dV signal at −80 mV. Contrast is adjusted for visibility. (e) dI/dV spectra on an isolated H_2Pc molecule (red) and a H_2Pc molecule within the quantum corral in (a) (black). (f) dI/dV spectra on an isolated Co adatom (red) and a Co adatom within a 10.1 nm radius quantum corral (black). (g) Diagram of the measurement where the magnetic impurity interacts with both the bulk and confined surface states of the substrate.

After preparing the magnetic impurities and confirming their Fano resonance signal with dI/dV spectroscopy, we proceeded to build the corrals from either Co or Ag adatoms. Individual Ag adatoms were dropped from the tip [13,40], and adatoms were manipulated laterally in constant-current mode ($V = 2$ mV, $I = 60$ nA). Figures 1(a) and 1(b) show two complete corrals, where the confined surface state electrons generate a characteristic bias-dependent standing wave pattern in the STM constant-current topography imaging mode. Low-bias dI/dV spectra (−80 to 80 mV) were acquired using lock-in amplification with $V_{\mathrm{mod}} < 2$ mV after stabilizing the tip height at 80 mV. Figures 1(c) and 1(d) show dI/dV spectra measured across the corral center, where the confined modes appear as peaks symmetrically around the corral center. The central magnetic impurity acts as a scattering potential for the surface state electrons, modifying the background signal of the confined modes. Figures 1(e) and 1(f) demonstrate how the low-energy spectra change within corrals compared to isolated impurities: the zero-bias anomaly not only is superimposed on the confined mode background but is expected to change in shape. Figure 1(g) illustrates the electronic

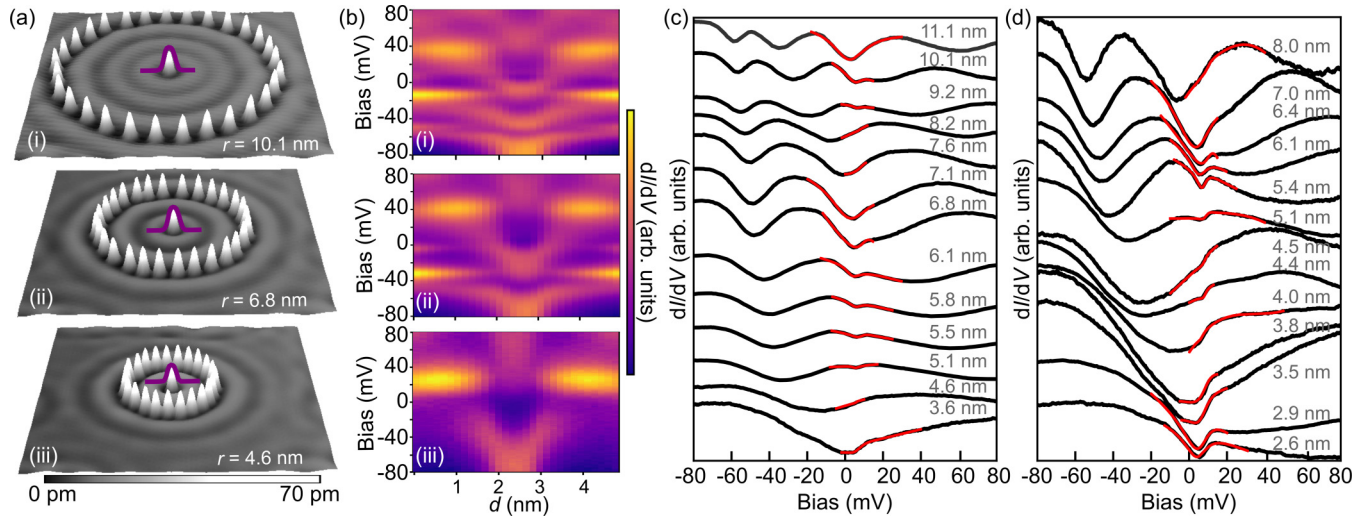

FIG. 2. (a) Constant-current topography of Co adatoms inside quantum corrals of radius r built from Ag adatoms. (b) dI/dV line spectra taken across Co adatoms in Ag corrals with radius r along the purple lines in (a). Spectra in panels (i), (ii), and (iii) were measured on the same Co atom, with no STM tip changes from manipulation procedures ($I = 1$ nA, $V_b = 80$ mV, $V_{\text{mod}} = 1$–2 mV). Representative dI/dV point spectra on Co adatoms in (c) Ag and (d) Co corrals with Fano fits overlaid in red. Fit bounds were selected so $\epsilon_0 \approx 7.1$ mV to match the value obtained for an isolated Co adatom [22,29] (see Fig. S6 in the SM [42] for interpolated spectra and fit values showing ϵ_0 as a function of r). Spectra are vertically offset for clarity. Typical measurement parameters are $I = 0.5$–1.5 nA, $V_b = 40$–1000 mV, and z offset of 0–1 Å.

environment of the magnetic impurity in a quantum corral. The density of states (DOS) at E_F is composed of bulk conduction bands and the surface states modulated by the corral confinement. Our measurements aimed to extract the Fano resonance signature and determine its evolution as a function of corral radius.

The low-energy conductance spectra of Co adatoms and H_2Pc molecules have typically been modeled with a Fano line shape [41]. Observed in tunneling spectra of various Kondo systems, the Fano line shape arises from interference between electron tunneling paths into a discrete level on the magnetic impurity and a continuum of electronic states in the metallic substrate. From a practical perspective, the parameters of a Fano fit can be used to characterize a zero-bias anomaly, regardless of its Kondo or spin excitation origin. The resulting line shape in dI/dV spectra is given by

$$dI/dV(\epsilon) = A\frac{(q+\zeta)^2}{1+\zeta^2} + B\epsilon + C, \tag{1}$$

where

$$\zeta = \frac{\epsilon - \epsilon_0}{\Gamma_0/2},$$

ϵ is the energy centered at E_F, ϵ_0 is the energy of the resonant level, q is the Fano parameter, Γ_0 is the resonance full width at half maximum, and A, B, and C are resonance amplitude and linear background coefficients, respectively. STS of isolated Co adatoms (H_2Pc molecules) on large Ag(111) terraces exhibits a Fano resonance line shape with $\epsilon_0 = 8$ meV (-2 meV), $\Gamma_0 = 8$ meV (11.2 ± 1.7 meV), and $q = 0.1$ ($\sim$20) [22,37]. Low-energy tunneling spectra can also vary slightly based on STM tip shape and the distance to other surface adatoms and step edges [29,37].

To remove effects of the varying surface state background [29], we kept the central impurity position constant and manipulated only the corral wall atoms to adjust the surface state density at the center of the corral. We first built the largest corral with the free wall atoms available on the surface, then measured point and line spectra on the central impurity. Then we used semiautomated atom manipulation scripts to measure the corral radius and create a corral slightly smaller than the current one (see the Supplemental Material (SM) [42]). Excess wall atoms were removed as necessary to prevent dimer formation and to keep the mean distance between adjacent wall adatoms smaller than $\lambda_{E_F}/2$ to control the scattering and confinement of surface state electrons via the corral walls. We built corrals at least 20 nm away from Ag(111) step edges to maintain surface state onset energy at the Co adatom near the nominal value of -67 mV (see Fig. S1 in the SM [42]) [22,43,44]. By building corrals with radii between 2.8 and 11 nm, the number of occupied corral eigenmodes was tuned from 0 to 17.

III. RESULTS AND DISCUSSION

A. Co adatoms in Co and Ag corrals

Figure 2(a) shows examples of the built corrals, line spectra measured across the central Co adatom, and point spectra on the Co adatom as a function of corral radius. With sufficiently small lock-in modulations and large current set points, the zero-bias anomaly is seen as a discontinuity close to $\sim$7.1 mV in most corrals. The spatial and energetic profile of the Co adatom bound state near -80 meV changes as a function of corral radius [Fig. 2(b)] as the Co adatom bound state partially overlaps with corral eigenmodes. This signifies modifications in hybridization with the surface band structure [45]. The amplitude of the Fano resonance decays approximately 0.5 nm from the center of the Co atom regardless of the corral size, consistent with theory [46] and previous experiments for Co/Cu(100) [27] and Co/Ag(111) [25]. Similar

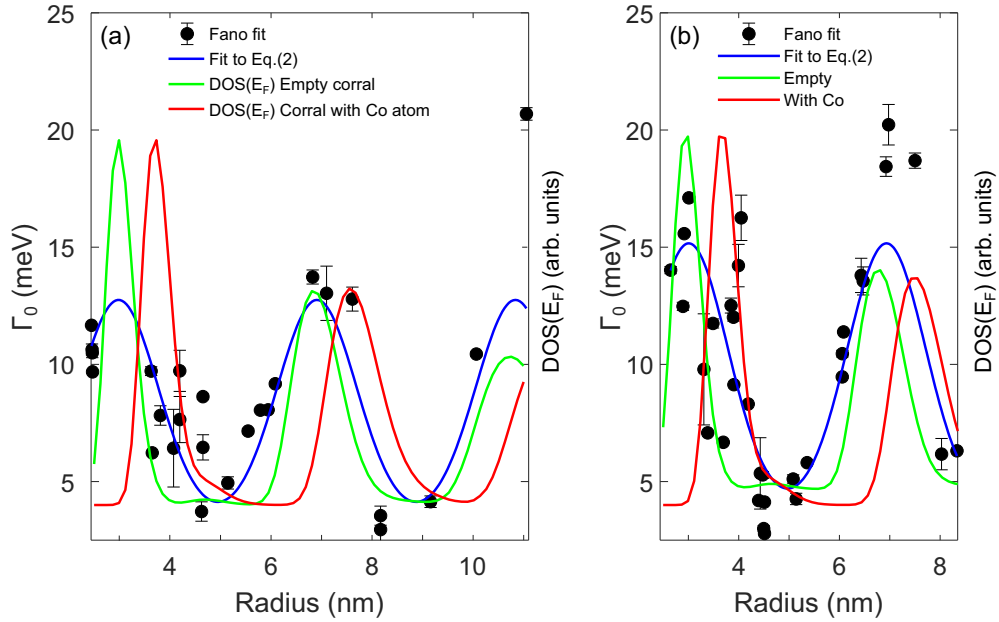

FIG. 3. Co adatom Fano resonance width as a function of corral radius for corrals with (a) Ag and (b) Co walls. Fits to Eq. (2) are overlaid in blue, and particle-in-a-box model estimates for LDOS at E_F are in red and green for occupied and empty corrals, respectively. Several spectra were measured on the same atom with different tips, and multiple corrals were built with similar radii. Error bars are estimated standard deviations from fit to 1. The central Co adatoms were positioned less than a lattice constant away from the fitted corral center point (see Fig. S12 in the SM).

spatial decay is observed by fitting Fano line shapes to spectra measured in a grid around a Co atom at the quantum corral center (see Fig. S4 in the SM [42]).

We fit the dI/dV spectra on the Co atoms in the corral centers with Fano line shapes and extract the widths Γ_0 as a function of corral radius. The results plotted in Fig. 3 display periodic variations in Γ_0. Earlier studies associated these variations with the confined modes varying the local DOS (LDOS) at E_F, but the models used to estimate the LDOS variations were based on empty corral structures [8,47]. The central atom is expected to "gate" the confined modes of a quantum corral [12], leading to increased confinement and shifting the eigenmode energies localized in the corral center. To assess the impact of this increased confinement, we performed particle-in-a-box calculations for empty corrals and ones occupied with a Co atom approximated as a disk potential [42]. The parameters needed to initialize the model were obtained from fits to line spectra across corral centers with a Co atom. The general shape of the variation is reproduced by both the empty and occupied corral calculations, but the Fano width data follow the empty corral estimate better. This can be rationalized in terms of the Ag(111) surface state dispersion and the resulting Fermi wavelength $\lambda_F \approx 2\pi/k_F \approx 75$ Å, which is significantly larger than the Co atom. This means the confined modes of an empty corral are an adequate approximation for the conduction bath environment of the Co atom. In any case, the significant changes in the Fano width can be understood as a consequence of DOS modulation at E_F due to the quantum confined modes in the corrals. Confined modes on the Co adatom can also be modeled by modifying the surface state dispersion parameters and corral radius (see Figs. S2 and S3 in the SM [42]).

In order to compare our results with previous results in the literature [22], we now estimate surface and bulk state exchange constants between Co and Ag(111) by using a model that incorporates the width Γ_0 as a function of corral radius r:

$$\Gamma_0 = D \exp\left(\frac{-1}{J_b\rho_b + J_s\rho_{s0}[1 + A\cos(2kr + \delta)]}\right). \quad (2)$$

We fix $\rho_{s0} = 0.125$ eV^{-1}, $\rho_b = 0.27$ eV^{-1}, and $D = 4.48$ eV in accordance with [22] and fit Eq. (2) to the extracted Fano widths Γ_0 for Co adatoms in corrals with Ag and Co walls. From the fit we extract exchange coupling energies $J_{s,b}$ and scattering phase shift δ. Several different fit models accurately reproduce the measured trend in the zero-bias anomaly width as a function of corral radius. Furthermore, some models reproduce the trend well but have large covariance between variables. We treat these models separately in the SM [42]. Fit results for the simplest model with $A = 1$ are compiled in Table I and visualized in Fig. 3.

Extracted exchange constants $J_{b,s}$ for Co/Ag(111) are consistent with those reported by Li *et al.* [22] for corrals built from both Co and Ag adatoms. We see variations in the Fano resonance energy ϵ_0 and asymmetry parameter q as a function of corral radius (see Fig. S6 in the SM [42]). For small corral

TABLE I. Model fit parameters for Co/Ag(111) data.

Parameter	Ag corrals	Co corrals
J_s (eV)	0.11 ± 0.02	0.12 ± 0.02
J_b (eV)	0.530 ± 0.013	0.54 ± 0.015
δ	1.511 ± 0.132	1.47 ± 0.14

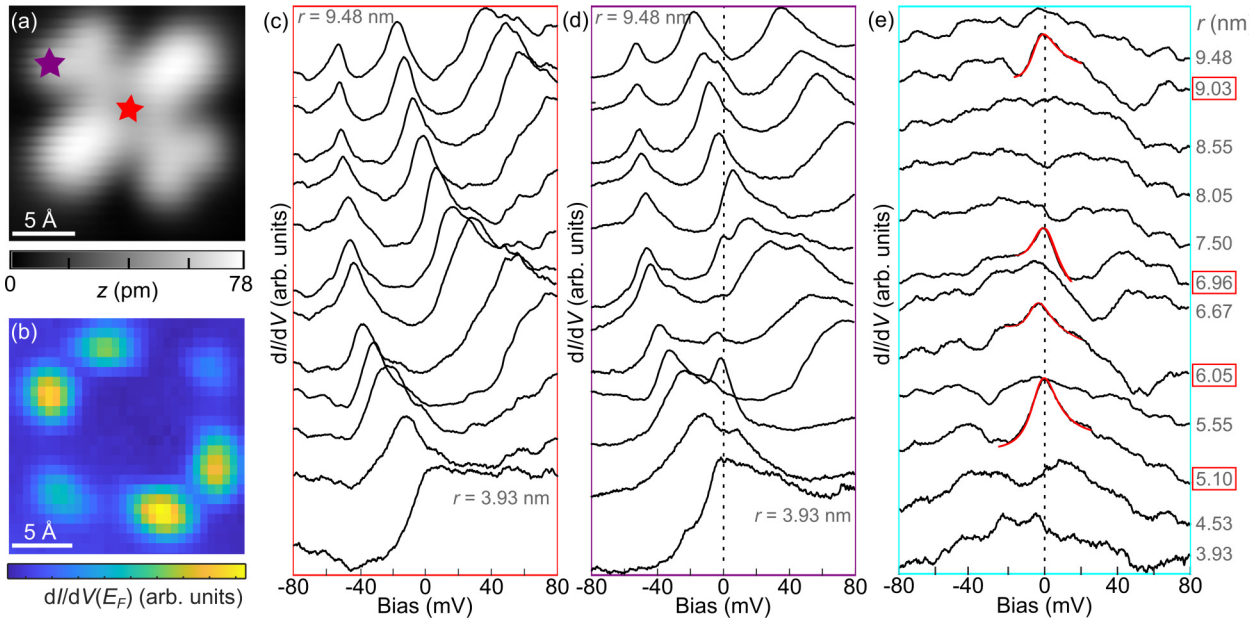

FIG. 4. (a) Constant-current topography of an isolated H_2Pc molecule ($I = 1$ nA, $V = 80$ mV). (b) Zero-bias conductance map of an isolated H_2Pc molecule. (c) dI/dV spectra taken at the center of H_2Pc molecules at the center of Ag adatom quantum corrals of radius r. (d) dI/dV spectra taken at the split lobe of H_2Pc molecules at the center of Ag quantum corrals of radius r. (e) dI/dV spectra from (d) with dI/dV spectra from (c) subtracted in order to better detect the Kondo resonance peak. Fano resonance fits are overlaid in red.

radius r, the choice of the corral wall adatom may affect the lifetime or spin polarization of surface state electrons coupled to the central impurity. Limot *et al.* reported that Ag adatoms alter Ag(111) surface state lifetime, whereas Co adatoms do not [45]. Surface state quasiparticle lifetimes impacted by the wall atom species may affect the amplitude of the resonance features seen on the central Co adatom [48]. Moro-Lagares *et al.* showed that the Fano resonance amplitude depends on the type of adatom in dimers and coupled chains on Ag(111), but none of the other resonance parameters do; only Co-Ag and Co-Co dimers within a distance less than six lattice sites showed any differences in Fano resonance amplitude [29]. For all our corrals, distances between the central and wall atoms were larger than distances at which an effect on the Fano resonance would be noticeable. In summary, as seen in Table I, we observe only the expected change in the scattering phase shift δ but no difference in either J_s or J_b between Ag and Co corrals.

The data presented here can be used for comparison with the recently proposed spinaron origin of the observed zero-bias anomaly. The observed width variation is significantly stronger than what would be expected if the features arose from simple spin-flip excitations of a higher spin magnetic impurity with nonzero magnetic anisotropy energy. The spinaron excitation, in contrast, is expected to be sensitive to the density of states of the corral due to the induced polarization in the bath. The spinaron model of magnetic impurities on Cu, Ag, and Au(111) surfaces suggests that the line shape should fit the Fano resonance (rather than, e.g., the Fano-Frota line shape [49]) and that the resonance should be shifted towards positive bias by several mV, in contrast to the classic Kondo resonance that is very close to E_F [34–36]. Interestingly, these criteria are fulfilled in the Co/Ag(111) system, yet predictions for the detailed variation of the resonance width with a change in the surface state DOS would require a full first-principles many-body treatment of this system.

B. H_2Pc molecules in Ag corrals

To establish whether the Kondo resonance of other magnetic impurities can be tuned via quantum confinement, we repeated the measurements with H_2Pc molecules inside corrals built from Ag adatoms. As shown in Fig. 4(b) , the Kondo resonance of an isolated H_2Pc molecule is localized on the frontier orbitals which hold the impurity spin. Local variations in Fano fit parameters of an isolated molecule were established from grid spectroscopy (see Fig. S5 in the SM [42]).

For the H_2Pc molecules inside the corrals, dI/dV spectra were measured along the "split lobe" direction across the molecule to characterize both the Kondo resonance and the confined modes (examples of spectra along a line across the molecule are shown in Fig. S7 in the SM [42]). Figures 4(c) and 4(d) show the dI/dV spectra measured at the molecule's center [red star in Fig. 4(a)] and on the split lobe [purple star in Fig. 4(a)] for varying corral radii. The expected Kondo peaks are not clearly distinguishable in most of the spectra on the split lobe due to the confined mode background and its spatial variations around E_F. In particular, there are modes with a node in the corral center that are not visible in the spectra shown in Fig. 4(c) but contribute to the features in Fig. 4(d) (see Fig. S8 in the SM [42]). Heat map plots of the line spectra show contrast close to E_F for many corrals, suggesting that the Kondo effect persists even if it is smeared by the confined modes (see Fig. S8 in the SM [42]). The dI/dV curves in Fig. 4(d) can be fitted well with four to eight Gaussians, but significant Kondo peaks do not stand out when

TABLE II. Fano fit parameters for H_2Pc molecules.

H_2Pc environment	Γ_0 (meV)	ϵ_0 (meV)	q (arb. units)
5.1 nm radius corral	17.1	−2.0	5.5
6.05 nm radius corral	16.1	−3.9	4.5
6.96 nm radius corral	15.3	0.5	32.8
9.03 nm radius corral	15.6	−4.8	2.0
Isolated	25.5	−2.4	7.2

comparing the fit results with particle-in-a-box calculations (see Fig. S9 in the SM [42]).

Spectra at the molecule's center were subtracted from the split lobe point spectra in order to minimize background DOS effects. Figure 4(e) shows the result of this subtraction: at certain radii, a peak at zero bias becomes visible. Fano line shapes were fitted to low-bias peaks in the subtracted point spectra. For radii $r = 6.05$ and 6.96 nm, the Kondo resonance does not overlap with the confined modes. For corral radii $r = 5.1$ and $r = 9.03$ nm, there are some contributions from local variations of confined modes across the molecule length, as indicated by particle-in-a-box modeling [42]; however, considering the spectral weight of the other confined modes that remain after the subtraction, we can still extract the Fano linewidth with sufficient confidence. For the rest of the corrals, quantitative extraction of the Fano parameters was not possible. Extracted fit parameters are shown in Table II.

Significant variations are visible in the width, energy position, and q factor across the different corral radii. The widths extracted are consistently smaller than those on isolated molecules, as in previous measurements on self-assembled monolayers [37]. Although the lack of visible Kondo peaks on most radii makes a fit to Eq. (2) impossible and thus the exchange constants cannot be extracted, the corral has a clear impact on the Kondo features compared to an isolated molecule.

The overall line shape and behavior are strikingly different compared to those of Co adatoms inside circular corrals, where the Fano dip is clearly distinguishable for most corral radii. The spin state, impurity orbital energies, and orbital overlaps with the conduction bands are markedly different between Co atoms and H_2Pc molecules, which should result in a different amplitude for the Fano width variation according to Eq. (2). In addition, it is likely that the zero-bias features correspond to spinaron excitation for the cobalt atom and a clean $S = 1/2$ Kondo effect for the H_2Pc molecules. A number of experimental factors could influence the observed width and precise shape of the H_2Pc Kondo peak, such as adsorption geometry [37], tip DOS [25], and instrument noise conditions [50]. We measured the Kondo signatures of an isolated H_2Pc molecule as a function of tip height and found only limited variation in the resulting Fano fit parameters (see Figs. S10 and S11 in the SM [42]). Therefore, variations in the tip height or the tip-molecule interaction do not explain the different radius dependence and suppressed Fano signatures compared to the Co atoms.

To probe the influence of confined modes on the H_2Pc Kondo resonance further, an accurate model of the confined mode energy widths and lifetimes on the molecule is required. Recent advances towards electron spin resonance STM on Ag surfaces [51] hold promise for exploring the magnetic properties of H_2Pc molecules in quantum corrals. Given the complexity uncovered in this system, further experiments with other Kondo impurities (such as triangulenes [52]) in quantum corrals and theoretical studies on their behavior may also be warranted.

IV. CONCLUSIONS

We showed the tunability of spinaron and Kondo excitations by probing individual magnetic impurities in atomically engineered quantum corrals. Our findings demonstrate the significance of the surface state in the low-energy spinaron and Kondo zero-bias anomalies of magnetic impurities adsorbed on Ag(111). We observed periodic variations in the zero-bias anomaly widths of Co/Ag(111) by modulating the surrounding surface state and extracted exchange constants consistent with those previously reported. These results confirm that the Co adatom zero-bias anomaly is coupled to the DOS at E_F and demonstrate qualitatively different behavior between the spinaron Co atom and Kondo H_2Pc molecules in the electronic environment generated by quantum corrals. Our findings establish a starting point to control spinaron and Kondo excitations via confinement engineering of an underlying conduction bath.

ACKNOWLEDGMENTS

We thank G. Chen, R. Drost, and X. Huang for assistance with the preliminary experiments and fruitful discussions. This research made use of the Aalto Nanomicroscopy Center (Aalto NMC) facilities and Aalto Research Software Engineering services. The authors acknowledge funding from the European Research Council (ERC-2017-AdG No. 788185, "Artificial Designer Materials," and ERC-2021-StG No. 101039500, "Tailoring Quantum Matter on the Flatland") and the Academy of Finland (Academy Professor Funding Grants No. 318995 and No. 320555 and Academy Research Fellow Grants No. 331342, No. 336243, No. 338478, and No. 346654).

M.A. and A.K. contributed equally to this work.

[1] J. Kondo, Resistance minimum in dilute magnetic alloys, Prog. Theor. Phys. **32**, 37 (1964).

[2] D. Goldhaber-Gordon, H. Shtrikman, D. Mahalu, D. Abusch-Magder, U. Meirav, and M. A. Kastner, Kondo effect in a single-electron transistor, Nature (London) **391**, 156 (1998).

[3] A. M. Chang and J. C. Chen, The Kondo effect in coupled-quantum dots, Rep. Prog. Phys. **72**, 096501 (2009).

[4] V. Madhavan, W. Chen, T. Jamneala, M. F. Crommie, and N. S. Wingreen, Tunneling into a single magnetic atom: Spectroscopic evidence of the Kondo resonance, Science **280**, 567 (1998).

[5] K. Nagaoka, T. Jamneala, M. Grobis, and M. F. Crommie, Temperature dependence of a single Kondo impurity, Phys. Rev. Lett. **88**, 077205 (2002).

[6] M. Ternes, A. J. Heinrich, and W. D. Schneider, Spectroscopic manifestations of the Kondo effect on single adatoms, J. Phys.: Condens. Matter **21**, 053001 (2009).

[7] Y. H. Zhang, S. Kahle, T. Herden, C. Stroh, M. Mayor, U. Schlickum, M. Ternes, P. Wahl, and K. Kern, Temperature and magnetic field dependence of a Kondo system in the weak coupling regime, Nat. Commun. **4**, 2110 (2013).

[8] M. F. Crommie, C. P. Lutz, and D. M. Eigler, Confinement of electrons to quantum corrals on a metal surface, Science **262**, 218 (1993).

[9] Q. Li, R. Cao, and H. Ding, Quantum size effect in nanocorrals: From fundamental to potential applications, Appl. Phys. Lett. **117**, 060501 (2020).

[10] C. R. Moon, L. S. Mattos, B. K. Foster, G. Zeltzer, W. Ko, and H. C. Manoharan, Quantum phase extraction in isospectral electronic nanostructures, Science **319**, 782 (2008).

[11] A. T. Ngo, E. H. Kim, and S. E. Ulloa, Single-atom gating and magnetic interactions in quantum corrals, Phys. Rev. B **95**, 161407(R) (2017).

[12] C. R. Moon, C. P. Lutz, and H. C. Manoharan, Single-atom gating of quantum-state superpositions, Nat. Phys. **4**, 454 (2008).

[13] J. Kügel, M. Leisegang, M. Böhme, A. Krönlein, A. Sixta, and M. Bode, Remote single-molecule switching: Identification and nanoengineering of hot electron-induced tautomerization, Nano Lett. **17**, 5106 (2017).

[14] S. W. Hla, K. F. Braun, B. Wassermann, and K. H. Rieder, Controlled low-temperature molecular manipulation of sexiphenyl molecules on Ag(111) using scanning tunneling microscopy, Phys. Rev. Lett. **93**, 208302 (2004).

[15] V. S. Stepanyuk, L. Niebergall, W. Hergert, and P. Bruno, *Ab initio* study of mirages and magnetic interactions in quantum corrals, Phys. Rev. Lett. **94**, 187201 (2005).

[16] H. C. Manoharan, C. P. Lutz, and D. M. Eigler, Quantum mirages formed by coherent projection of electronic structure, Nature (London) **403**, 512 (2000).

[17] Q. Li, X. Li, B. Miao, L. Sun, G. Chen, P. Han, and H. Ding, Kondo-free mirages in elliptical quantum corrals, Nat. Commun. **11**, 1400 (2020).

[18] S. N. Kempkes, M. R. Slot, S. E. Freeney, S. J. M. Zevenhuizen, D. Vanmaekelbergh, I. Swart, and C. M. Smith, Design and characterization of electrons in a fractal geometry, Nat. Phys. **15**, 127 (2019).

[19] S. N. Kempkes, M. R. Slot, J. J. van den Broeke, P. Capiod, W. A. Benalcazar, D. Vanmaekelbergh, D. Bercioux, I. Swart, and C. Morais Smith, Robust zero-energy modes in an electronic higher-order topological insulator, Nat. Mater. **18**, 1292 (2019).

[20] K. K. Gomes, W. Mar, W. Ko, F. Guinea, and H. C. Manoharan, Designer Dirac fermions and topological phases in molecular graphene, Nature (London) **483**, 306 (2012).

[21] A. A. Khajetoorians, D. Wegner, A. F. Otte, and I. Swart, Creating designer quantum states of matter atom-by-atom, Nat. Rev. Phys. **1**, 703 (2019).

[22] Q. L. Li, C. Zheng, R. Wang, B. F. Miao, R. X. Cao, L. Sun, D. Wu, Y. Z. Wu, S. C. Li, B. G. Wang, and H. F. Ding, Role of the surface state in the Kondo resonance width of a Co single adatom on Ag(111), Phys. Rev. B **97**, 035417 (2018).

[23] J. Henzl and K. Morgenstern, Contribution of the surface state to the observation of the surface Kondo resonance, Phys. Rev. Lett. **98**, 266601 (2007).

[24] L. Limot and R. Berndt, Kondo effect and surface-state electrons, Appl. Surf. Sci. **237**, 572 (2004).

[25] M. Moro-Lagares, J. Fernández, P. Roura-Bas, M. R. Ibarra, A. A. Aligia, and D. Serrate, Quantifying the leading role of the surface state in the Kondo effect of Co/Ag(111), Phys. Rev. B **97**, 235442 (2018).

[26] M. A. Schneider, L. Vitali, P. Wahl, N. Knorr, L. Diekhöner, G. Wittich, M. Vogelgesang, and K. Kern, Kondo state of Co impurities at noble metal surfaces, Appl. Phys. A **80**, 937 (2005).

[27] N. Knorr, M. A. Schneider, L. Diekhöner, P. Wahl, and K. Kern, Kondo effect of single Co adatoms on Cu surfaces, Phys. Rev. Lett. **88**, 096804 (2002).

[28] J. Ren, H. Guo, J. Pan, Y. Y. Zhang, X. Wu, H.-G. Luo, S. Du, S. T. Pantelides, and H.-J. Gao, Kondo effect of cobalt adatoms on a graphene monolayer controlled by substrate-induced ripples, Nano Lett. **14**, 4011 (2014).

[29] M. Moro-Lagares, R. Korytár, M. Piantek, R. Robles, N. Lorente, J. I. Pascual, M. R. Ibarra, and D. Serrate, Real space manifestations of coherent screening in atomic scale Kondo lattices, Nat. Commun. **10**, 2211 (2019).

[30] S. Fölsch, P. Hyldgaard, R. Koch, and K. H. Ploog, Quantum confinement in monatomic Cu chains on Cu(111), Phys. Rev. Lett. **92**, 056803 (2004).

[31] J. Figgins, L. S. Mattos, W. Mar, Y. T. Chen, H. C. Manoharan, and D. K. Morr, Quantum engineered Kondo lattices, Nat. Commun. **10**, 5588 (2019).

[32] P. W. Anderson, Localized magnetic states in metals, Phys. Rev. **124**, 41 (1961).

[33] A. Valli, M. P. Bahlke, A. Kowalski, M. Karolak, C. Herrmann, and G. Sangiovanni, Kondo screening in Co adatoms with full Coulomb interaction, Phys. Rev. Res. **2**, 033432 (2020).

[34] J. Bouaziz, F. S. Mendes Guimarães, and S. Lounis, A new view on the origin of zero-bias anomalies of Co atoms atop noble metal surfaces, Nat. Commun. **11**, 6112 (2020).

[35] F. Friedrich, A. Odobesko, J. Bouaziz, S. Lounis, and M. Bode, Evidence for spinarons in Co adatoms, Nat. Phys. **20**, 28 (2024).

[36] N. Noei, R. Mozara, A. M. Montero, S. Brinker, N. Ide, F. S. M. Guimarães, A. I. Lichtenstein, R. Berndt, S. Lounis, and A. Weismann, Manipulating the spin orientation of Co atoms using monatomic Cu chains, Nano Lett. **23**, 8988 (2023).

[37] J. Granet, M. Sicot, I. C. Gerber, G. Kremer, T. Pierron, B. Kierren, L. Moreau, Y. Fagot-Revurat, S. Lamare, F. Chérioux, and D. Malterre, Adsorption-induced Kondo effect in metal-free phthalocyanine on Ag(111), J. Phys. Chem. C **124**, 10441 (2020).

[38] J. Homberg, A. Weismann, R. Berndt, and M. Gruber, Inducing and controlling molecular magnetism through supramolecular manipulation, ACS Nano **14**, 17387 (2020).

[39] D. G. de Oteyza and T. Frederiksen, Carbon-based nanostructures as a versatile platform for tunable π-magnetism, J. Phys.: Condens. Matter **34**, 443001 (2022).

[40] L. Limot, J. Kröger, R. Berndt, A. Garcia-Lekue, and W. A. Hofer, Atom transfer and single-adatom contacts, Phys. Rev. Lett. **94**, 126102 (2005).
[41] U. Fano, Effects of configuration interaction on intensities and phase shifts, Phys. Rev. **124**, 1866 (1961).
[42] See Supplemental Material at http://link.aps.org/supplemental/10.1103/PhysRevB.109.195415 for more spectra, Fano fit parameters, a data repository, and analysis code, which includes Refs. [8,53–59].
[43] M. A. Schneider, L. Vitali, N. Knorr, and K. Kern, Observing the scattering phase shift of isolated Kondo impurities at surfaces, Phys. Rev. B **65**, 121406(R) (2002).
[44] Q. L. Li, R. Wang, K. X. Xie, X. X. Li, C. Zheng, R. X. Cao, B. F. Miao, L. Sun, B. G. Wang, and H. F. Ding, Green's function approach to the Kondo effect in nanosized quantum corrals, Phys. Rev. B **97**, 155401 (2018).
[45] L. Limot, E. Pehlke, J. Kröger, and R. Berndt, Surface-state localization at adatoms, Phys. Rev. Lett. **94**, 036805 (2005).
[46] M. Plihal and J. W. Gadzuk, Nonequilibrium theory of scanning tunneling spectroscopy via adsorbate resonances: Nonmagnetic and Kondo impurities, Phys. Rev. B **63**, 085404 (2001).
[47] J. Kliewer, R. Berndt, and S. Crampin, Controlled modification of individual adsorbate electronic structure, Phys. Rev. Lett. **85**, 4936 (2000).
[48] J. Fernández, M. Moro-Lagares, D. Serrate, and A. A. Aligia, Manipulation of the surface density of states of Ag(111) by means of resonators: Experiment and theory, Phys. Rev. B **94**, 075408 (2016).
[49] H. O. Frota, Shape of the Kondo resonance, Phys. Rev. B **45**, 1096 (1992).
[50] M. Gruber, A. Weismann, and R. Berndt, The Kondo resonance line shape in scanning tunnelling spectroscopy: Instrumental aspects, J. Phys.: Condens. Matter **30**, 424001 (2018).
[51] T. Esat, M. Ternes, R. Temirov, and F. S. Tautz, Electron spin secluded inside a bottom-up assembled standing metal-molecule nanostructure, Phys. Rev. Res. **5**, 033200 (2023).
[52] E. Turco, A. Bernhardt, N. Krane, L. Valenta, R. Fasel, M. Juríček, and P. Ruffieux, Observation of the magnetic ground state of the two smallest triangular nanographenes, JACS Au **3**, 1358 (2023).
[53] P. Wahl, M. A. Schneider, L. Diekhöner, R. Vogelgesang, and K. Kern, Quantum coherence of image potential states, Phys. Rev. Lett. **91**, 106802 (2003).
[54] H. Jensen, J. Kröger, R. Berndt, and S. Crampin, Electron dynamics in vacancy islands: Scanning tunneling spectroscopy on Ag(111), Phys. Rev. B **71**, 155417 (2005).
[55] J. Kliewer, R. Berndt, and S. Crampin, Scanning tunnelling spectroscopy of electron resonators, New J. Phys. **3**, 22 (2001).
[56] O. Újsághy, J. Kroha, L. Szunyogh, and A. Zawadowski, Theory of the Fano resonance in the STM tunneling density of states due to a single Kondo impurity, Phys. Rev. Lett. **85**, 2557 (2000).
[57] Y. Nagaoka, Self-consistent treatment of Kondo's effect in dilute alloys, Phys. Rev. **138**, A1112 (1965).
[58] M. Weiss, F. Stilp, A. J. Weymouth, and F. J. Giessibl, Revealing a spatially inhomogeneous broadening effect in artificial quantum structures caused by electron-adsorbate scattering, arXiv:2304.06571.
[59] N. Oinonen, C. Xu, B. Alldritt, F. F. Canova, F. Urtev, S. Cai, O. Krejčí, J. Kannala, P. Liljeroth, and A. S. Foster, Electrostatic discovery atomic force microscopy, ACS Nano **16**, 89 (2022).